Results in Engineering 25 (2025) 103735

Contents lists available at ScienceDirect

Results in Engineering

journal homepage: www.sciencedirect.com/journal/results-in-engineering

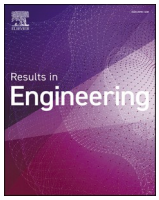

Experimental investigation and theoretical prediction of sleeve reinforced PGFRP composite under flexural loading for cross-arm application

Vijayvignesh Namasivayam Sukumaar [a,*], Mohamad Ridzwan Ishak [a,b,c,*], Mohd Na'Im Abdullah [a], Mohamed Yusoff Mohd Zuhri [c,d], Muhammad Asyraf Muhammad Rizal [e,f]

[a] Department of Aerospace Engineering, Universiti Putra Malaysia, 43400 UPM Serdang, Selangor, Malaysia
[b] Aerospace Malaysia Research Centre (AMRC), Universiti Putra Malaysia, 43400 UPM Serdang, Selangor, Malaysia
[c] Laboratory of Biocomposite Technology, Institute of Tropical Forestry and Forest Products (INTROP), Universiti Putra Malaysia, 43400 UPM Serdang, Selangor, Malaysia
[d] Advanced Engineering Materials and Composites Research Centre (AEMC), Department of Mechanical and Manufacturing Engineering, Universiti Putra Malaysia, 43400 UPM Serdang, Selangor, Malaysia
[e] Engineering Design Research Group, Faculty of Mechanical Engineeting, Universiti Teknologi Malaysia, 81310 Johor Bahru, Johor, Malaysia
[f] Centre for Advanced Composite Materials (CACM), Universiti Teknologi Malaysia, 81310 Johor Bahru, Johor, Malaysia

ARTICLE INFO

Keywords:
Cross-arm
Elastic moduli
Flexural properties
Pultruded glass fibre composite
Sleeve reinforcement

ABSTRACT

Pultruded glass fibre reinforced polymer composite is used as a cross-arm material in high-rise transmission tower application to suspend insulators, conductor cables and vibration dampeners. Due to long-term static loading conditions, they fail due to incompetency in the cross-arm's mechanical properties. This study establishes a feasible method to improve the service life by retrofitting a sleeve reinforcement, sandwiching the composite fastened by bolting, to strengthen the overall structure. This study is focused, at the coupon scale level, to determine the influence of this structural element upon the elastic mechanical properties under instantaneous and creep load conditions. The composite material and the stainless steel sleeve are fabricated using waterjet machining and laser cutting respectively. A comparative study among the virgin and varying lengths of sleeve reinforced composite is established for homogenizing this concept at the actual scale applications. It has been observed that the composite reinforced with the sleeve of 100% length as that of the composite specimen showed enhancement in its flexural elastic moduli by about 178% and 138% under instantaneous and creep load conditions as compared to its virgin counterpart. The Findley numerical model in compliance with creep results was used to generate equations to predict the deterioration of mechanical properties. This data helps to determine the functional service life of the composite in actual application. The sleeve installation has been found to increase the bending strength thereby resulting in reduced strain and promoting localized encapsulation, resilience, toughness, load transfer capability and creep strain resistance of the PGFRP composite.

1. Introduction

Nowadays, in Malaysia, the electricity consumption in modern metropolitan areas accounts for about 75% of total power consumption, which is required to run the industrial and residential sectors to fulfil everyday population needs [1]. As a result, high voltage transmission towers must be constructed by energy companies to provide consumers with sufficient electricity. A tower with a tall-latticed steel structure is used to raise and uphold various components of the transmission line systems [2,3]. The majority of transmission towers, in a variety of sizes and designs, are constructed using composite materials, hardwood lumber and galvanized steel. Three primary working lines, at 132, 275, and 500 kilovolts (kV), are used by these towers to accommodate the electrical supply from 420 sub-stations [4]. A transmission tower consists of structural components that are integrated into the peak, cage, tower body and cross-arms. The cross-arm, as illustrated in Fig. 1, is one of the most important part of the transmission tower. It is an extended assembly made up of multiple long arm components that are used to

* Corresponding authors.
E-mail addresses: n.s.vijayvignesh@gmail.com (V.N. Sukumaar), mohdridzwan@upm.edu.my (M.R. Ishak), naimabdullah@upm.edu.my (M.N. Abdullah), zuhri@upm.edu.my (M.Y.M. Zuhri), muhammadasyraf.mr@utm.my (M.A.M. Rizal).

https://doi.org/10.1016/j.rineng.2024.103735
Received 27 September 2024; Received in revised form 3 December 2024; Accepted 12 December 2024
Available online 13 December 2024

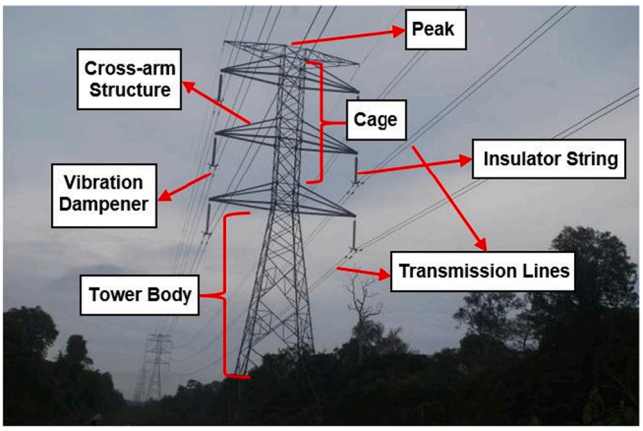

Fig. 1. Cross-arm assembly in a transmission tower.

support overhead electrical utility lines.

Chengal wood was used to construct the cross-arms of a 132 kV suspension tower since 1963. However, the scarcity of hardwood lumber and the deterioration of wood over time have made it necessary to discover new substitutes [5,6]. Given that the wooden cross-arm is made of natural fibre, it showed signs of natural wood faults when subjected to high humidity and continuous stress over an extended period of time [7–12]. Therefore, a study proposed that a comprehensive strategy be used to replace the wooden cross-arms in the Malaysian electrical grid system with other alternatives, like glass fibre reinforced polymer (GFRP) composite material [5]. The combination of E-glass fibre and unsaturated polyester resin, exhibited promising qualities, performance and manufacturability for large construction applications [13]. Numerous studies demonstrate the widespread usage of glass fibre reinforced polymer composite in a variety of structural industries, such as wind turbines, bridge decks, retrofitting beams and structural fasteners [14–17]. The composite is composed of fine fibres, which have the advantages of being stiff, lightweight and mechanically strong while requiring less raw materials and energy during manufacturing [18–21]. Recent studies also focus upon the utilization of natural fibres or a combination of natural and synthetic fibres for structural applications due to their sustainable advantages [22]. It has been experimentally proven that the combination of kenaf and glass fibres have yielded not just desirable mechanical properties but also superior creep and fatigue responses prolonging the service life in real-world conditions [23]. However, the major drawbacks still exists in their inherent phenomenon of being deteriorated due to water absorption, thermal ageing and quicker yielding, which make them unsuitable for implementation in the current applications [24].

Compared to hardwood lumber, pultruded glass fibre reinforced polymer composites are relatively new in cross-arm applications, thus the research on enhancing their long-term durability by utilization of structural reinforcements is still in its early stages. Also, the utilization of sleeves have so far found its application as a temporary repair mechanism but never as a preventive measure to resist rupture and catastrophic failure. To address these research gaps, it is mandatory to characterize their behaviour in real-time conditions, that is, to perform a profiling on long-term mechanical testing (creep) upon the coupon scale specimen as its experimental origin. The outcome of this study is anticipated to indicate the applicability and functional capability of the additional installation made to obtain desired results. A three-point flexural testing mode is used in a coupon scale experiment to assess the virgin and the bolted sleeve reinforced cross-arms made of pultruded glass fibre reinforced polymer composite material. The mechanical qualities would be assessed using these tests in terms of compression and shearing activities [13,25]. This mode's bending impact is realizable and resembles the in-service cross-arm of a transmission tower's cantilever beam mode [26]. Better comprehension and the ability to forecast the materials' service life can be observed from the creep pattern found from cross-arm materials [20,27]. Thus, before proceeding on to a full-scale cross-arm structure, this study would establish an initial and thorough examination for the material used as cross-arm.

A traditional style of testing (load-based test) was carried out for 1,000 hours. The observed creep trends can be further expanded and enhanced with the use of accessible numerical modelling. The most commonly used numerical models are Burger model, Findley power law model and Bailey-Norton model [28–31]. However, it has been validated that the Findley power law model is most suitable for implementation of studies related to cross-arms in transmission tower application [14,32,33]. These models help scientists and engineers forecast the material's time-dependent, long-term features through empirical formulations using power-based approaches or through practical dashpot-spring element applications.

In this work, an instantaneous and long-term mechanical flexural testing were conducted using coupon scale virgin and bolted sleeve strengthened pultruded glass fibre reinforced polymer composite cross-arms, to compare and characterize the quasi-static creep and flexural properties in real time scenario. In several literatures, glass fibre reinforced polymer composite have been shown to have superior mechanical qualities [14,34]. However, a comparative analysis of the long-term mechanical characteristics of virgin and structurally reinforced cross-arm material is still lacking. The purpose of this study is to estimate quasi-static behaviours and creep trends in order to validate the material and the proposed sleeve reinforcement for the cross-arms, which are ideal for use in transmission tower applications. As a result, it helps in understanding the functional role of structural reinforcements upon composite materials in similar demanding applications. This article also emphasizes upon the applicability of the creep model to describe the creep strain of sleeve retrofitted pultruded glass fibre reinforced polymer composite cross-arms in coupon scale size. Finally, the research also creates a general equation to forecast creep response.

2. Methods

This research study is broken down into two phases: experimental activities and numerical analyses. The subsequent sections explain the research's specific procedures and techniques in detail.

2.1. Materials

The coupon scale specimens of cross-arm material were made of pultruded glass fibre reinforced polymer composite, comprising of 37% volume fraction of E-glass fibre and 63% volume fraction of unsaturated polyester resin, obtained from Electrius Sendirian Berhad, Selangor, Malaysia. The coupon scale specimen size, are 124.8 mm long, 31.2 mm wide and 7.8 mm thick with a length-to-thickness ratio of 16:1 as per ASTM D790 standards [14,35]. Table 1 provides information on the mechanical properties and laminate structure of the pultruded glass fibre reinforced polymer composite used in the current study respectively.

The stacked fibre laminate raster orientation, from the outermost to

Table 1
Mechanical properties of PGFRP composite [36,37].

Property	PGFRP composite
Density	2580 kg/m^3 – E-glass 1350 kg/m^3 – Unsaturated polyester
Texture	Fine, homogenously and unidirectional fibre along the matrix
Shrinkage	Low
Natural Durability	Low
Modulus of Elasticity	29.8 GPa
Modulus of Rupture	858.0 MPa

the innermost ply, is 45°/-45°/0°/90°/45° corresponding to the ply thickness of 0.5/0.5/0.7/3.6/0.7 mm respectively with the remaining thickness of 1.8 mm being filled by the matrix symmetrically [38,39]. These specimens are cut to desired dimensions from the full-scale cross-arm structure by the utilization of waterjet machining, to avoid heat generation, in order to prevent deterioration of the mechanical properties. The sleeve reinforcement used are made of stainless steel SS304 obtained from Tan Central Metal (Kuala Lumpur) Sendirian Berhad, Selangor, Malaysia. Their dimensions were cut to 47.2 mm wide, 2 mm thick with a varying length as a percentage, in steps of 10%, of the span length of the coupon scale cross-arm, namely 50%, 60%, 70%, 80%, 90%, 100% whose equivalent dimensions are 62.4 mm, 74.9 mm, 87.4 mm, 99.8 mm, 112.3 mm and 124.8 mm respectively. The composite is sandwiched using symmetrical steel plates and are fastened together using SS304 M4 bolts, with a length of 16 mm, and nuts obtained from Hua Hui, Zhongshan, China.

The retrofitted sleeve lengths are considered starting from 50% as that of the span length of the composite specimen and lesser lengths are neglected due to its inefficiency in enhancing structural integrity. As the load is induced, the maximum stress occurs at the mid-point of the specimen but the critical stress corresponding to failure occurs over a region upon the surface [40]. This phenomenon has more pronounced effects when subjected to long-term creep conditions. The shortest length of structural reinforcement corresponds to 8 times the thickness of the base material under deformation, which in this case with the specimen thickness of 7.8 mm corresponds to 50% of the composite length [41]. In order to overcome such drastic scenarios, the capability of stress transfer has to be enhanced which thereby leads to neglecting sleeve lengths less than half of the composite specimen due to their negligible influence [42].

The sleeves are cut to dimensions, holes of 4 mm diameter are made at an symmetrical equidistance of 10 mm using laser cutting technique. This specific equidistance is used based on the generic condition that the distance between the hole distance must be greater than at least 2.2 times the nominal diameter of the bolt to ensure uniform concealing pressure upon the sandwiched composite specimen. whose assembled structure is illustrated in Fig. 2. The torque used to tighten the bolts to form structure is 2.5 Nm, since SS304 M4 bolt-nut are used, which have a critical maximum permissible torque of 3 Nm. The process of tightening is done at a slower pace to ensure the avoidance of galling. The torque wrench is used to ascertain the imparted torque thereby producing a strong bond capable of inducing negligible slip potential. Mitutoyo 2050A Japan, analog dial gauges were used to measure deflections produced under loads, supported using the magnetic holders. The relative temperature and humidity of the open environment were measured using the thermo-hygrometer. OriginPro V10.1 computer software is used to evaluate the Findley numerical model.

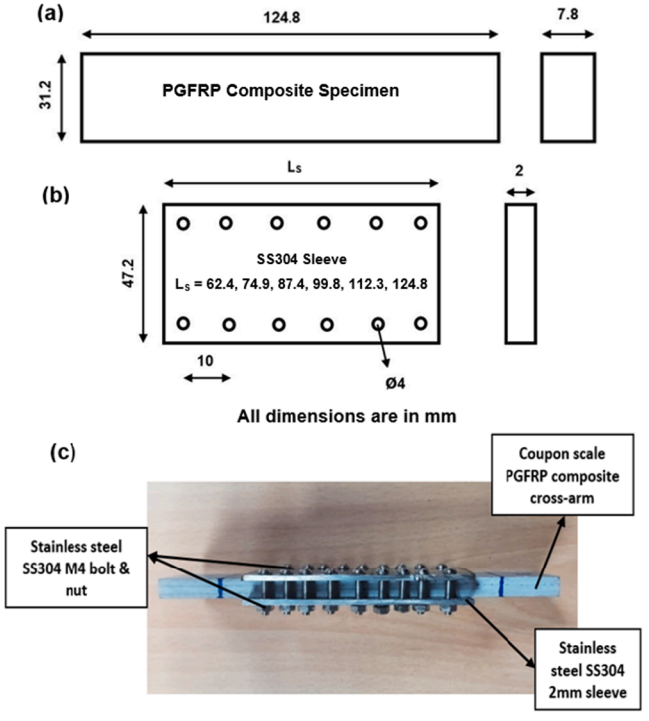

Fig. 2. Coupon scale (a) PGFRP composite dimensions (b) SS304 sleeve dimensions (c) assembled test specimen.

2.2. Flexural load-deflection

In a quasi-static flexural test, the values of flexural strength and modulus for virgin and sleeve installed pultruded glass fibre reinforced polymer composite specimens were obtained by averaging five repetitions. The examination was carried out based on ASTM D790, an international testing standard. The flexural load-deflection is performed within the elastic limit, to co-relate with real-time scenarios, upon the specimens that are endured to a maximum load of 1760 N, determined using the static flexural loading until failure, corresponding to 40% load of ultimate flexural stress (UFS). This load parameter was identified by introducing the specimens through short-term flexural tests using an INSTRON Universal Testing Machine (UTM) with a nose fixture and support diameter of 250 mm. The bending properties of virgin pultruded glass fibre reinforced polymer composite was assessed under the instantaneous loading effect at a loading speed of 3.33 mm/min in the flexural test [14]. The elastic flexural load-deflection test performed is used to identify parameters, namely, elastic flexural stress, elastic flexural strain and elastic flexural modulus of the specimens using Eqs. (1), (2) and (3) respectively [43].

$$\sigma = \frac{3Fl}{2bh^2} \tag{1}$$

where, σ represents elastic flexural stress in N/mm^2, F represents load induced in N, l represents the span length of the specimen in mm, b represents breadth of the specimen in mm, h represents the thickness of the specimen in mm.

$$\epsilon = \frac{6\delta h}{l^2} \tag{2}$$

where, ϵ represents elastic flexural strain, δ represents deflection produced in mm.

$$E_{flex} = \frac{Fl^3}{4b\delta h^3} \tag{3}$$

where, E_{flex} represents elastic flexural modulus. Since, the loading is done within the elastic limits; the elastic flexural modulus is same as that of Young's modulus (E) of the material.

In addition to elastic longitudinal mechanical properties, the elastic lateral mechanical properties, namely, elastic flexural shear stress, elastic flexural shear strain and elastic shear modulus can also be found out using Eqs. (4), (5) and (6) respectively [44].

$$\sigma_s = \frac{3F}{2bh} \tag{4}$$

where, σ_s represents elastic flexural shear stress in N/mm^2.

$$\epsilon_s = \frac{d^2\delta}{2yl}$$

where, d represents the distance from the neutral axis to the point of application of load in mm and y represents the distance from the neutral axis to the point of interest in mm. However in this case, the neutral axis

is the mid-point so $d = h/2$ and the point of consideration is the outermost layer such that $y = d = h/2$. Hence, the above equation becomes,

$$\epsilon_s = \frac{h\delta}{4l} \tag{5}$$

$$S_{flex} = \frac{\sigma_s}{\epsilon_s} \tag{6}$$

where, S_{flex} represents elastic flexural shear modulus in N/mm^2. Since, the loading is done within the elastic limits; the elastic shear flexural modulus is same as that of rigidity modulus (G) of the material.

2.3. Flexural creep

The flexural creep test upon the virgin and sleeve fastened pultruded glass fibre reinforced polymer composite were performed as per the international testing standard ASTM D2990. Based on the standard, each specimen were induced to long-term constant loading for 1000 hours in an open environment wherein the deformation values were obtained at intervals of 0, 0.1, 0.2, 0.5, 1, 2, 5, 20, 50, 100, 200, 500, 700 and 1000 hours sequentially. 15 seconds after the working tension was applied, the first strain, also referred to as the "immediate or instantaneous strain", was measured. The creep mechanical properties of the specimens were obtained by averaging three repetitions at three varying load levels. These loads were split into three consecutive values within the elastic limit, corresponding to the ultimate flexural strength (UFS) of virgin pultruded glass fibre reinforced polymer composite, which are 10%, 20% and 30% respectively [14].

To measure the deflection value, the dial gauges were placed at the top of the loading hook supported by the magnetic holders. The experimental procedure was executed at tropical environmental condition to mimic the real-time operational conditions. In Malaysia, there exists no seasonal changes and entire year is experienced by alternating sunny or rainy days within a standard range of temperature and humidity. Increase in either one of these physical phenomena results in reduction of flexural modulus of the composite, that is, inversely proportional [45, 46]. These constantly varying conditions also results in alternating elongation and contraction of the composite, which acts like a localized cyclic loading resulting in a higher rate failure [47]. These physical parameters directly affect the flexural loading by imparting changes in the capability of stress distribution, material's resistance to bending and other surface deteriorations eventually leading to reduction in desirable mechanical properties [48]. Thus, investigation in actual scenario and the effect of sleeve reinforcement ascertains the efficiency and the novelty of the current study

The coupon scale specimens are mounted upon the test rig with a loading hook whose inward face is welded with a cylindrical solid bar. This bar acts as the contact interface between the loading hook and the composite specimen, through which the induced load is imparted upon the specimens. The region of contact of the bar is a line along the mid-section of the specimen, perpendicular to the length of the specimen, in compliance with ASTM flexural testing standards. The load is induced along the vertical axis via the suspended fixture to hold slots, hung in-line with the axis of the solid bar. The dial gauge is positioned vertically above the loading hook at the mid-point, which helps determine the deflection produced, when the load is engaged without any deviations such as coupling due to eccentric loads or offset axes. Prior to the initiation of the experiment, all the specimens were stored under room temperature for over a month and the entire measurement tools were calibrated. The coupon scale experimental setup for execution of flexural load-deflection and flexural creep studies are illustrated in Fig. 3.

The creep specimens were coded, in order, C, P hyphenated with S, that is CP-S, which stand for pultruded glass fibre reinforced polymer composite, percentage value of constant loading (10 = 10% of UFS, 20 = 20% of UFS, 30 = 30% of UFS) and percentage of sleeve length (0 = 0% (virgin), 50 = 50%, 60 = 60%, 70 = 70%, 80 = 80%, 90 = 90%, 100 = 100% of span lengths of the composite) respectively. This creep experiment is conducted to identify creep mechanical properties and their variation with respect to time thereby to observe actual functionality. The overall detail of the creep parameters are tabulated in Table 2 whose

Table 2
Creep test parameters.

Set	Specimen Type (CP_s)	Duration (Hours)	No. of each specimen	Load (N)
1.	C10-0, C10-50, C10-60, C10-70, C10-80, C10-90, C10-100	1000	3	436
2.	C20-0, C20-50, C20-60, C20-70, C20-80, C20-90, C20-100	1000	3	872
3.	C30-0, C30-50, C30-60, C30-70, C30-80, C30-90, C30-100	1000	3	1308

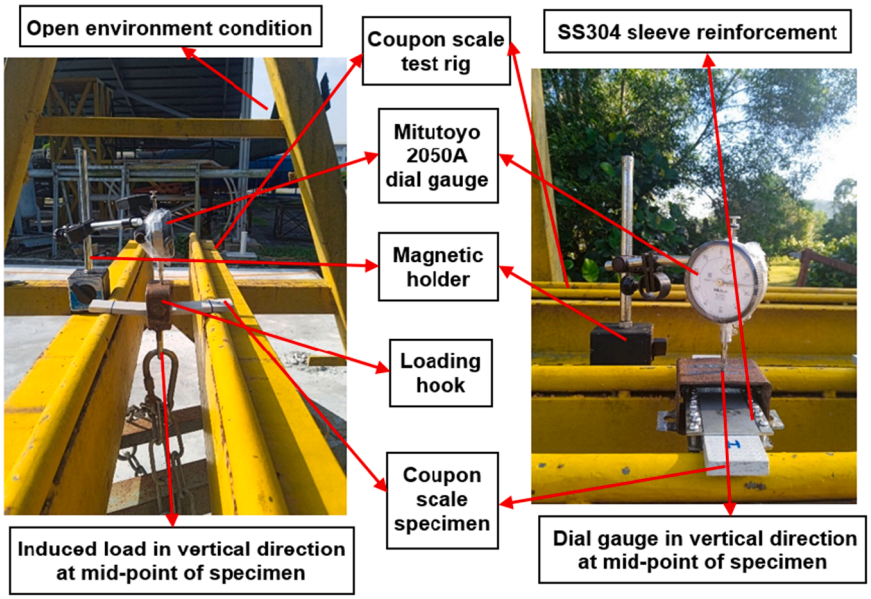

Fig. 3. Coupon scale experimental test setup.

load parameters are obtained from study [14].

The stress-strain relation of the creep study is observed to follow Hooke's law, hence the Young's modulus is found out using Eq. (7) [49].

$$E = \frac{\sigma}{\epsilon} \tag{7}$$

A measurement called creep compliance expresses a material's long-term resilience in terms of strain per unit stress. It is comprehensible mathematically as determined using Eq. (8) [50].

$$J(t) = \epsilon(t)/\sigma_0 \tag{8}$$

where, $J(t)$ represents creep compliance in MPa^{-1}, $\epsilon(t)$ represents strain, dependent upon time and σ_0 represents constant stress applied in MPa.

2.4. Validation model

In general there exists a few numerical models to validate creep data, one such is the physical model called as Burger model, which consider the parameters of elastic and viscoelastic moduli to predict the behaviour of the material subjected to steady state creep [28]. The Burger model comprises of three major component such as a linear elastic spring, a dash-pot, and the Kelvin-Voight element (a dash-pot along with a combination of dashpots and springs) [51,52].These components use elastic strain, permanent strain and viscoelastic strain to explain the creep behaviour. Usually, the tension acts at the displacement tip, resulting in an immediate strain. However, this model has been proven to be not suitable for the service life prediction of composite materials due to the model's unfair assumption of linear relationship with time and viscosity of the material [26]. Further, this model failed by predicting a steady decrease in the creep rate with time that resulted from their relationship assumption to be a constant rather than as a dependent variable [14,53].

Yet another numerical model employed for the creep study is Norton-Bailey model that evaluates the primary and secondary creep under a constant stress and temperature within the given time period [29]. Although this model is suitable for elaborating the transient creep of the material derived through the analysis of the steady-state creep response, this model cannot efficiently fit responses for longer durations [27,31]. In addition, the scope of this model lies only when the experiment is performed within the controlled conditions with no major deviations in temperature, which completely contradicts the current work wherein real-time working conditions are employed. Over long durations, the deviation from a positive to a negative fitting of obtained data has been proven by experiments upon the composite specimens [14].

The empirical numerical model termed as Findley model can overcome the drawbacks of the above said models. Findley model can be employed to find long-term creep responses based on the early creep strain data [54]. The parameters of this model is purely based on the actual engineering parameters without having any limitations upon the physical conditions and hence can validate the creep responses from the current work effectively. Any influence from the physical conditions are accounted for in the obtained experimental responses, as the evaluation is done based on the integrated outcomes, rather than based on an independent parameter or an induced constraint. The results obtained from creep experiments are validated using the Findley power law is proven to be most suitable and feasible for implementation upon the creep behavior of anisotropic materials [14,32,33] that can be determined using Eq. (9) [55].

$$\textit{Total Strain} = \textit{Elastic Strain} + \textit{Transient Strain}$$

$$\epsilon(t) = \epsilon_0 + at^b \tag{9}$$

where, ϵ_0 represents instantaneous strain, $\epsilon(t)$ represents strain at a particular time t, a represents stress-dependent coefficient and b represents stress-independent material constant wherein the values of a and b can be obtained by incorporating non-linear curve fitting technique in OriginPro software.

3. Results and discussions

3.1. Load-deflection behaviour

The load-deflection values were measured using the dial gauges at mid-point of the coupon scale pultruded glass fibre reinforced polymer composite specimens with and without sleeve reinforcement along its vertical axis as shown in Fig. 3. The average of load-deflection value was obtained by repeating each measurement five times. Fig. 4 shows the load-deflection response of both the virgin and sleeve strengthened pultruded glass fibre reinforced polymer composite. It is evident that the sleeved pultruded glass fibre reinforced polymer composite deforms less than its virgin counterpart under the same loading pattern. As long as there are minor deviations and no yielding of the composite material, this relationship holds true [56,57]. In view of this phenomenon, the pultruded glass fibre reinforced polymer composite is regarded as a linear elastic material that complies with Hooke's Law. More specifically, as the length of the sleeve reinforcement increases the deformation produced upon loading decreases. This is due to the reinforcement's capability to resist deflection and its ability to withstand greater stress. Additionally, the connected sleeve arrangement improves load transfer capabilities, which in turn serves to reduce the critical stress concentration zone thereby avoiding catastrophic failure by mechanizing the stress distribution across a greater region.

Under the same loads, it was found that the initial deflection of reinforced composite followed a pattern identical to that of virgin composite. One possible explanation for this could be that the effect of reinforcement comes into play only when the composite reaches a specific sagging point. This characteristic makes it easier to comprehend how the span of the sleeve reinforcement contributes to improved mechanical properties because the structural reinforcement does not experience reaction forces at the support elements during the initial loading stages of the composite. In addition, this mechanism helps to encapsulate that particular region endured to critical stress when induced to mechanical loading without any constraints upon its degrees of freedom.

Fig. 5 shows the longitudinal elastic flexural stress-strain plot of both the virgin and sleeve fastened pultruded glass fibre reinforced polymer composite. In order to examine its reactions in real-world operating conditions, the load induced is within the elastic limits. The sleeved

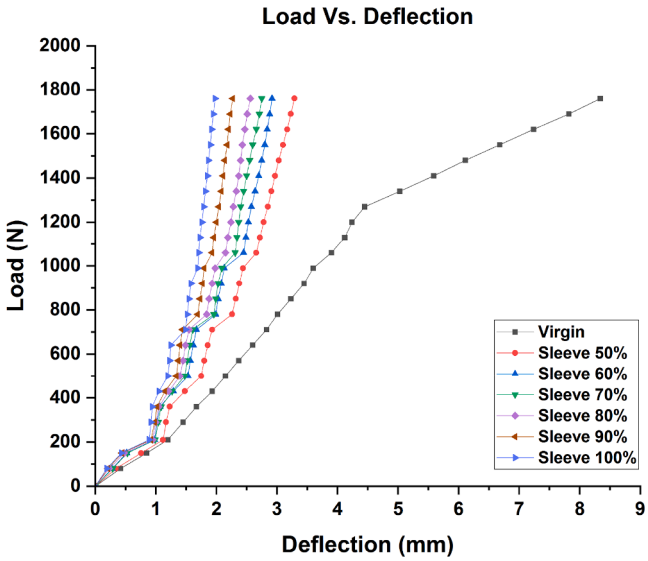

Fig. 4. Load-deflection plots of virgin and sleeve reinforced PGFRP composite.

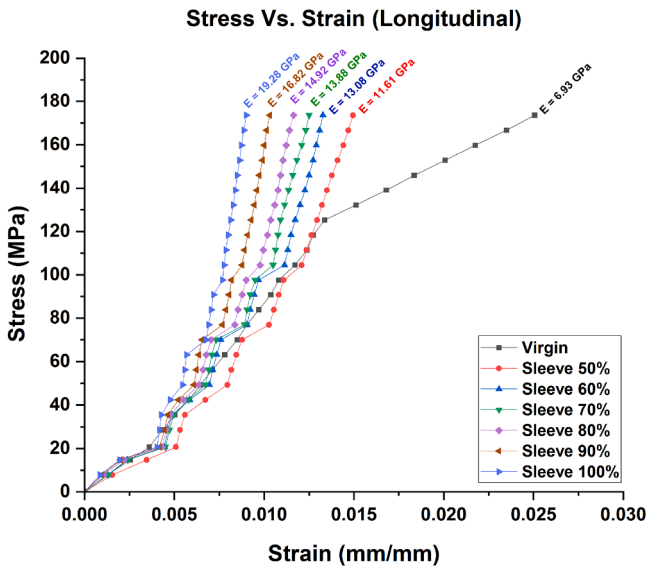

Fig. 5. Longitudinal stress-strain plots of virgin and sleeve reinforced PGFRP composite.

pultruded glass fibre reinforced polymer composite exhibits a lower strain than the virgin composite, with the concept of direct proportionality with the sleeve length. This is because the addition of sleeve reinforcement, which is able to withstand deformation and absorb more energy before breaking when subjected to stress, has increased the toughness of the structure. The incorporated structural element has demonstrated to have increased the region's transition resistance factor from elastic to plastic, owing to the newer structure's higher resilience to withstand hiked strain energy.

Thus, the elastic region of the structurally reinforced composite had greatly increased in comparison to its virgin counterpart, according to the comparative analysis plot of stress-strain of virgin and sleeved pultruded glass fibre reinforced polymer composite. It has been proven that the glass fibre in the unsaturated polyester (UPE) resin prevented the early onset of failure due to the compatibility of the matrix and the reinforcement [58,59]. Likewise, the installed structural reinforcement has further enhanced this compatibility by altering the components to enact as a single structure with the desirable advantages each element to resist deformation and to promote load distribution properties.

Eqs. (2) and (3) calculates the elastic flexural strain and modulus respectively, in the longitudinal axis, for virgin and varying lengths of sleeve retrofitted pultruded glass fibre reinforced polymer composites at the maximum elastic load limit of 1760 N that yields a constant stress of 173.57 MPa as per Eq. (1), are tabulated in Table 3. Within elastic bounds in the longitudinal axis, the structural reinforcement with a lengths of 50%, 60%, 70%, 80%, 90% and 100% of the composite span length has increased the pultruded glass fibre reinforced polymer composite's flexural modulus and, as a result, its resistance to bending under load by 67.53%, 88.74%, 100.29%, 115.30%, 142.71% and 178.21% respectively. Since the loading condition was within the elastic limit, the Young's modulus and the elastic flexural modulus are equivalent.

Table 3
Elastic flexural parameter values (longitudinal).

Specimen (PGFRP)	Strain	Modulus (GPa)
Virgin	0.0251	6.93
Sleeve 50%	0.0150	11.61
Sleeve 60%	0.0133	13.08
Sleeve 70%	0.0125	13.88
Sleeve 80%	0.0116	14.92
Sleeve 90%	0.0103	16.82
Sleeve 100%	0.0090	19.28

Fig. 6 shows the lateral stress-strain graph for both the virgin and sleeve reinforced composite. It is clearly seen that the lateral faces of the pultruded glass fibre reinforced polymer composite is subjected to lesser stress than the longitudinal faces. On the lateral axis of the composite, the sleeve reinforcement does significantly improve the elastic mechanical characteristics. This insight guarantees that sleeve reinforcement can be implemented on the actual-scale pultruded glass fibre reinforced polymer composite cross-arms. Conversely, the pultruded glass fibre reinforced epoxy composite used in the experiment had better bending capabilities than the glass fibre reinforced epoxy composite carried out by other studies [60]. This might be the result of the pultrusion procedure, which induced the glass fibre to maximum wettability with the resin to prevent the creation of voids in the composite laminate [61]. Therefore, the bending qualities (strength and modulus) of utilized composite and SS304 sleeve materials have substantial value to be used in transmission tower and for other related heavy construction applications.

According to Eqs. (5) and (6), the elastic flexural strain and modulus, in the transverse axis, of the virgin and varying lengths of sleeve reinforced composites are tabulated in Table 4, for the induced stress of 10.85 MPa calculated using Eq. (4). Within elastic bounds in the lateral axis, the structural reinforcement with a lengths of 50%, 60%, 70%, 80%, 90% and 100% of the composite span length has increased the pultruded glass fibre reinforced polymer composite's flexural modulus and, as a result, its resistance to bending under load by 67.47%, 89.16%, 101.20%, 115.66%, 143.37% and 179.52% respectively. The rigidity modulus and the flexural shear modulus are equivalent since the loading was within the elastic limit. Two observable facts account for these high modulus values: first, there exists no direct loading on the lateral faces of the composite; second, the bulk phenomenon, which is caused by the manufacturing process, causes load transfer to occur primarily in the direction of the glass fibre reinforcement, or the path of least resistance.

3.2. Creep behaviour

Fig. 7 shows the strain rate graphs of the virgin and varying length of sleeve reinforced composite at three different load levels. All the specimens showed an increase in creep strain as the load levels increased. The curves demonstrated that throughout 1000 hours of creep operation, there were two phases, elastic and viscoelastic zones. An anisotropic material, such as polymeric composite, exhibits elastic behaviour initially, followed by viscoelastic conditions, before entering the plastic

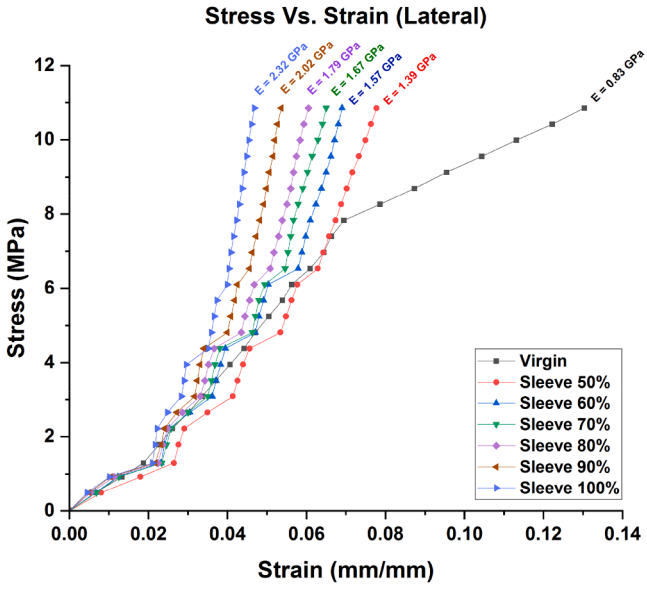

Fig. 6. Lateral stress-strain plots of virgin and sleeved PGFRP composite.

Table 4
Elastic flexural parameter values (lateral).

Specimen (PGFRP)	Strain	Modulus (GPa)
Virgin	0.1303	0.83
Sleeve 50%	0.0778	1.39
Sleeve 60%	0.0690	1.57
Sleeve 70%	0.0650	1.67
Sleeve 80%	0.0605	1.79
Sleeve 90%	0.0537	2.02
Sleeve 100%	0.0468	2.32

zone [62].

The indicated arrow in Fig. 7 suggests that the sleeve fastened pultruded glass fibre reinforced polymer composite in this experiment transitioned from the elastic period to the constant viscoelastic state more slowly than the virgin composite. This demonstrated that the structural reinforcement, as opposed to virgin material, promoted a more stable viscoelastic condition for cross-arm application. It is also observed that this region of viscoelasticity is directly proportional to the length of the sleeve reinforcement. After loading the specified weight for 15 seconds, the initial strain was measured. This assessment was carried out to categorize the degree of immediate strain. There was less creep strain in the improved pultruded glass fibre reinforced polymer composite with sleeve reinforcement than in the virgin material. This was caused by the fabric interlayer contact mechanism, which increased the strength of the structure by allowing the final layer of composite to overlap with the upper layer of the sleeve structure in the presence of a bolt and nut fastening mechanism [63]. Overall, the structural integrity had found to be increased by the installation of sleeve structures. Similar responses were found upon thin-walled aluminum tubes strengthened with carbon fibre reinforced polymer which has proven to increase their resistance to lateral crushing which thereby also enhances their capability absorb higher impact energies [64].

Fig. 7 is a plot between the creep strain (obtained by the ratio of deflection produced to the span length of the composite) and the time. The creep mode has three stages before rupture, namely primary, secondary and tertiary. However, since the loading is done within the elastic limit the tertiary stage is not attained. The primary stage is a completely elastic state and over time, under the influence of constant stress, the secondary stage is reached via the transition state. The initial

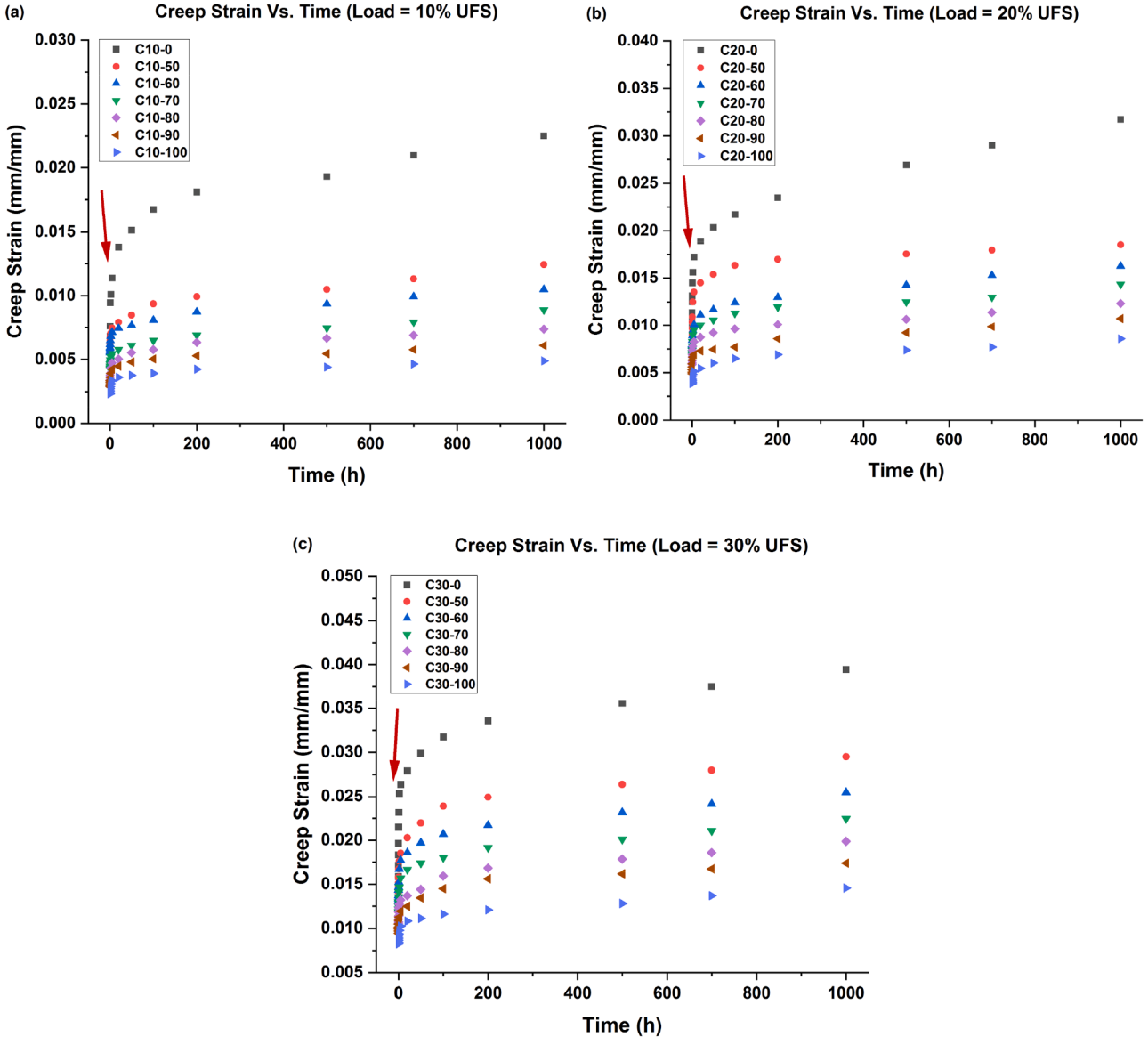

Fig. 7. Comparison of creep strain rate of virgin and varying lengths of sleeve reinforced PGFRP composite at (a) 10% (b) 20% (c) 30% load levels of ultimate flexural strength (UFS).

gap seen in the plot corresponds to the instantaneous elastic strain. The stronger the viscoelastic state (secondary creep stage) of a material during the creep, higher is its functional service life, whose transition initiation is indicated by the red arrow in the figure. It can be seen that at all load levels, the sleeve reinforced composite transits from the elastic to viscoelastic state at much lower creep strain indicating higher transient creep elastic flexural modulus that resists bending deformation by promoting stress distribution. It can also be seen that there exists a direct proportionality in fostering a stronger viscoelastic stage with the increase in the reinforced sleeve length. The increased creep strains experienced by the virgin composite, especially at the transition phase, indicates that there exists acute stress concertation that eventually leads to quicker failure. Numerically it can be seen that for a given constant load, for instance say at Load = 30% UFS, the elastic to viscoelastic transition initiation for virgin and 100% sleeve reinforced composite occurs at a creep strain of about 0.0025 mm/mm and 0.0010 mm/mm respectively, indicating an increase in the effectiveness of the sleeve reinforcement to prevent rupture by about 60%.

Additionally, at the same stress level, the sleeve reinforced composite experienced less creep strain than the virgin counterpart. According to this observation, the pultruded glass fibre reinforced polymer composite's intrinsic qualities, namely its unsaturated polyester matrix's good compatibility with glass fibre to facilitate stress transfer and enhance bending performance is found to have further enhanced by the structural sleeve reinforcement [65]. It is also observed that the sleeve length and the region of encapsulation are inversely proportional to the creep strain denoting the improvement in the resistance to deformations. Fig. 8 shows the relative temperature-humidity data experienced during the testing period mimicking real-time tropical conditions for about 1000 h in the open area with the average surrounding temperature (ST) of 29.5°C and relative humidity (RH) of 71.1 %.

Eq. (7) was used to identify the specimens' Young's moduli at different load levels using the idea of Hooke's Law. The average of these values was determined and is noted in Table 5. The average Young's modulus of sleeve strengthened pultruded glass fibre reinforced polymer composite of lengths 50%, 60%, 70%, 80%, 90% and 100% are found to be 12.01%, 22.76%, 41.72%, 70.04%, 96.46% and 138.05% respectively higher than that of virgin composite. The specimen's stiffness, resistance to deformation under load, and capacity for energy absorption and stress transmission under long-term static loading circumstances are all suggested by the specimen's improved Young's modulus.

The virgin and varying lengths of sleeve reinforced composite specimens time-dependent compliance plots are illustrated in Fig. 9. The stability of the material's creep performance was revealed by the

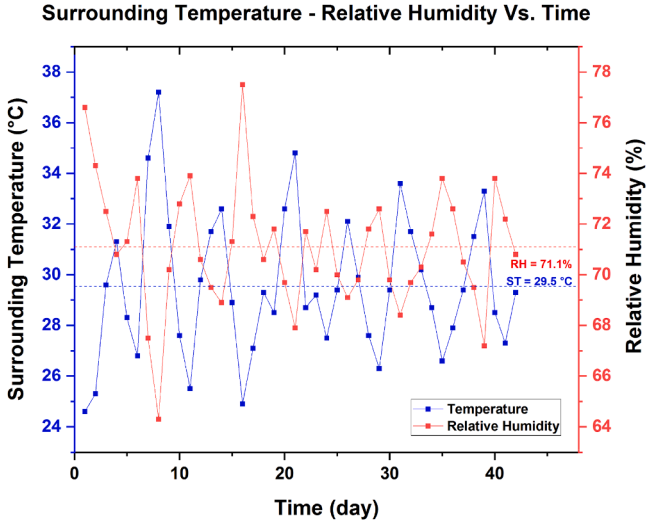

Fig. 8. Average temperature and relative humidity of open environment.

Table 5
Initial Young's modulus identification based on Hooke's law.

Specimen	Stress (MPa)	Initial Strain (x 10^{-3})	Initial Young's Modulus (GPa)	Average Initial Young's Modulus (GPa)
C10-0	42.99	6.25	6.88	7.91
C20-0	85.99	9.86	8.72	
C30-0	128.99	15.86	8.13	
C10-50	42.99	6.01	7.15	8.86
C20-50	85.99	8.37	10.27	
C30-50	128.99	14.10	9.15	
C10-60	42.99	5.53	7.77	9.71
C20-60	85.99	7.45	11.54	
C30-60	128.99	13.14	9.82	
C10-70	42.99	4.25	10.12	11.21
C20-70	85.99	6.81	12.63	
C30-70	128.99	11.86	10.88	
C10-80	42.99	3.19	13.48	13.45
C20-80	85.99	5.85	14.69	
C30-80	128.99	10.58	12.19	
C10-90	42.99	2.79	15.41	15.54
C20-90	85.99	4.89	17.58	
C30-90	128.99	9.46	13.64	
C10-100	42.99	2.32	18.53	18.83
C20-100	85.99	3.85	22.33	
C30-100	128.99	8.25	15.64	

uniformity of the creep compliance results for three replications of each specimen under three different stress levels. The intended result was achieved when the data demonstrated that the sleeve installed pultruded glass fibre reinforced polymer composite specimen exhibited much less creep compliance than the virgin composite for three successive load levels and also comply with the physical sleeve length criteria, that is, direct proportional relationship. This was ascribed to the sleeve reinforcement's robust structural bonding, which eliminated any possibility of slippage, and its compatibility with the composite, which contained synthetic resin (unsaturated polyester) and homogeneous E-glass fibre [66,67]. The pultruded glass fibre reinforced polymer composite reinforced by a sleeve structure increased the composite's bending strength. This improvement comes from the applied load being distributed between the more stiff fibre bundles enclosed within the sleeve structure and the flexible matrix of the composite [68].

The increase in creep compliance in virgin composite can be attributed to the structural deterioration of the cell wall components, as a result of the samples being exposed to continuously varying weather conditions throughout the day [69,70]. This can cause the propagation of micro cracks between the fibres and fibre pull-off due to the increasing stress magnitude [71]. Primary creep was reduced in the sleeved pultruded glass fibre reinforced polymer composite specimen because its bending strength was greater than that of its virgin counterpart. Structurally improved composites are often better at slowing down the creep rate than virgin composites, extending the material's service life and enabling it to support a constant load. Furthermore, the outcomes of these research could be extended to analyze effect of sleeve reinforcement upon their localized loading point, deformation of sub-surfaces, energy absorption characterizes and thin plate buckling phenomena [72].

3.3. Creep numerical model

The Findley numerical model was incorporated to the creep experimental data for validation whose plots along with the numerically defined equations are illustrated in Fig. 10. The fitted parameters from Eq. (9) are summarized in Table 6.

Due to the better steady-state creep response, it was found that the sleeve reinforced composite exhibited lesser transient creep coefficient '*a*', than the virgin composite. Although the pultruded glass fibre reinforced polymer composite had previously demonstrated to hold a higher level of resistance to creep, it appears that adding a sleeve reinforcement

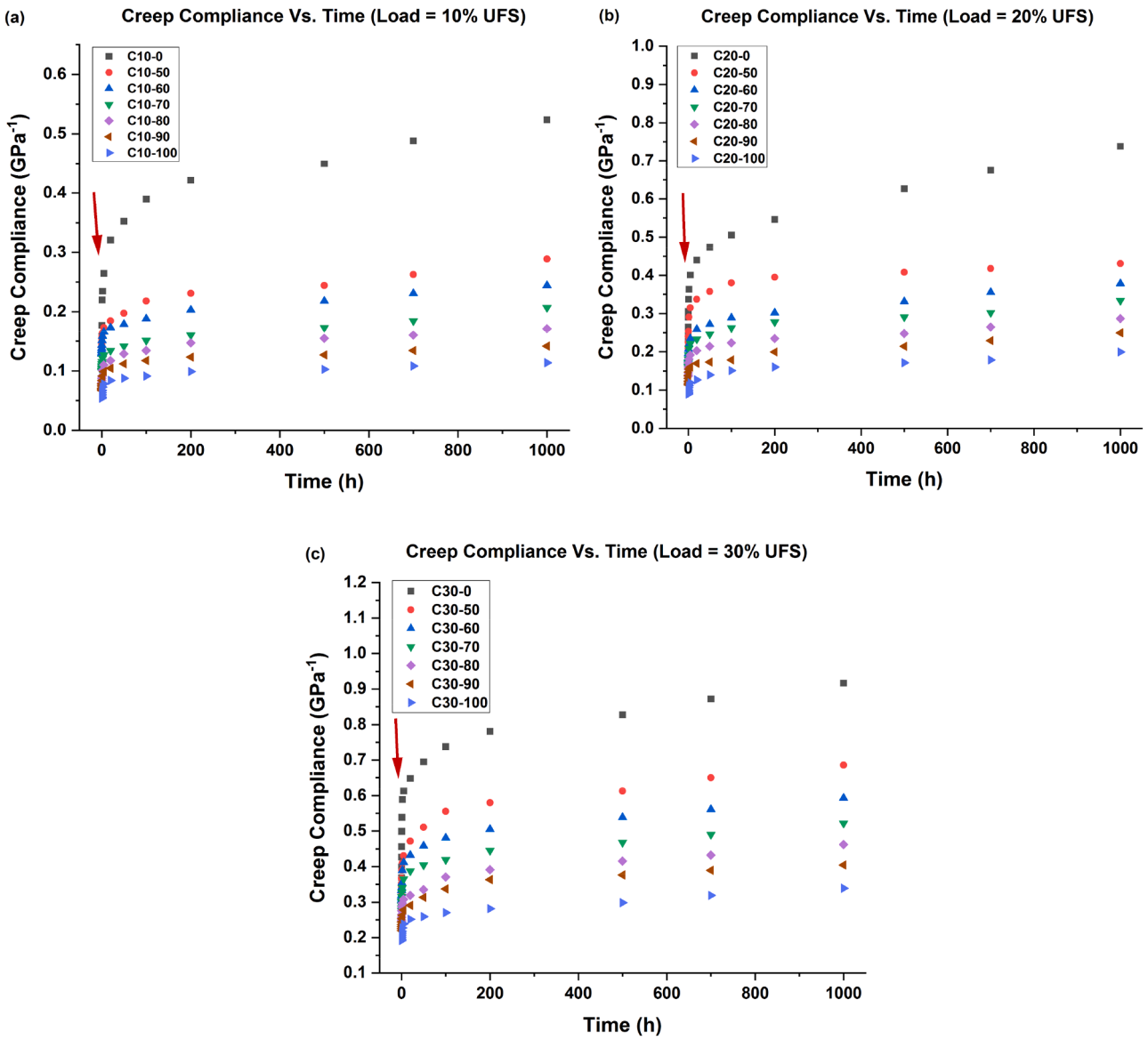

Fig. 9. Creep compliance against time of virgin and varying lengths of sleeve reinforced PGFRP composite at (a) 10% (b) 20% (c) 30% load levels of ultimate flexural strength (UFS).

to the composite would not have an effect on the secondary stage of creep [73,74]. The first creep of inelastic flow is represented by this transient creep strain, which gradually diminishes until the steady state period is attained [75]. In addition, both the virgin and sleeved composite's stress independent exponent '*b*', fell within the typical range of stress-independent material exponents [76–78].

Table 6 also summarizes the initial elastic flexural modulus ($E_{e,0}$) and transient creep flexural modulus (E_t) have been derived from the Findley model. The elastic flexural modulus helps in identifying the bending strength, durability under sustained loads and stress transfer capabilities that have a direct impact upon the failure of the composite. The transient creep flexural modulus determines the strength of the composite to resist deformation under rapid strain rate for the overall transition period as a cumulative data. The average of these derived parameters is possible as the entire loading is done within the elastic limits and provides overall moduli corresponding to the defined limits at various load intervals. It can be seen that both the elastic moduli are directly proportional to the length of the sleeve reinforcement. The transient creep for sleeve reinforced composite with lengths 50%, 60%, 70%, 80%, 90% and 100% has found to be increased by 60.54%, 66.54%, 72.40%, 72.54%, 75.74% and 83.56% respectively as compared to its virgin counterpart. The compliance of Findley numerical model with the experimental responses can be ascertained based on the initial elastic flexural modulus as similar to that done based on the instantaneous elastic strain values as done in Table 7.

It can be observed that the *Adj.* R^2 values of both the specimens at various load levels are in the range of 0.9720-0.9907 fostering a stronger reliability region of acceptance as validated by previous study [14]. The creep trend explained the steady-state creep behaviour in the secondary phase, making Findley's power law model the best numerical model to assess the creep performance of pultruded glass fibre reinforced polymer composite [31,79]. By contrasting each specimen's instantaneous strain values with the experimental instantaneous strain, it was further assessed and verified. Based on the ideas of Hooke's law, which stipulate that the value of instantaneous stress be linearly related to the stress that is induced. The validation of creep behavior conducted for the above mentioned specimens for further involved a comparison between the initial elastic strain derived from experimental data and empirical Findley's model which are tabulated in Table 7 along with their error percentage.

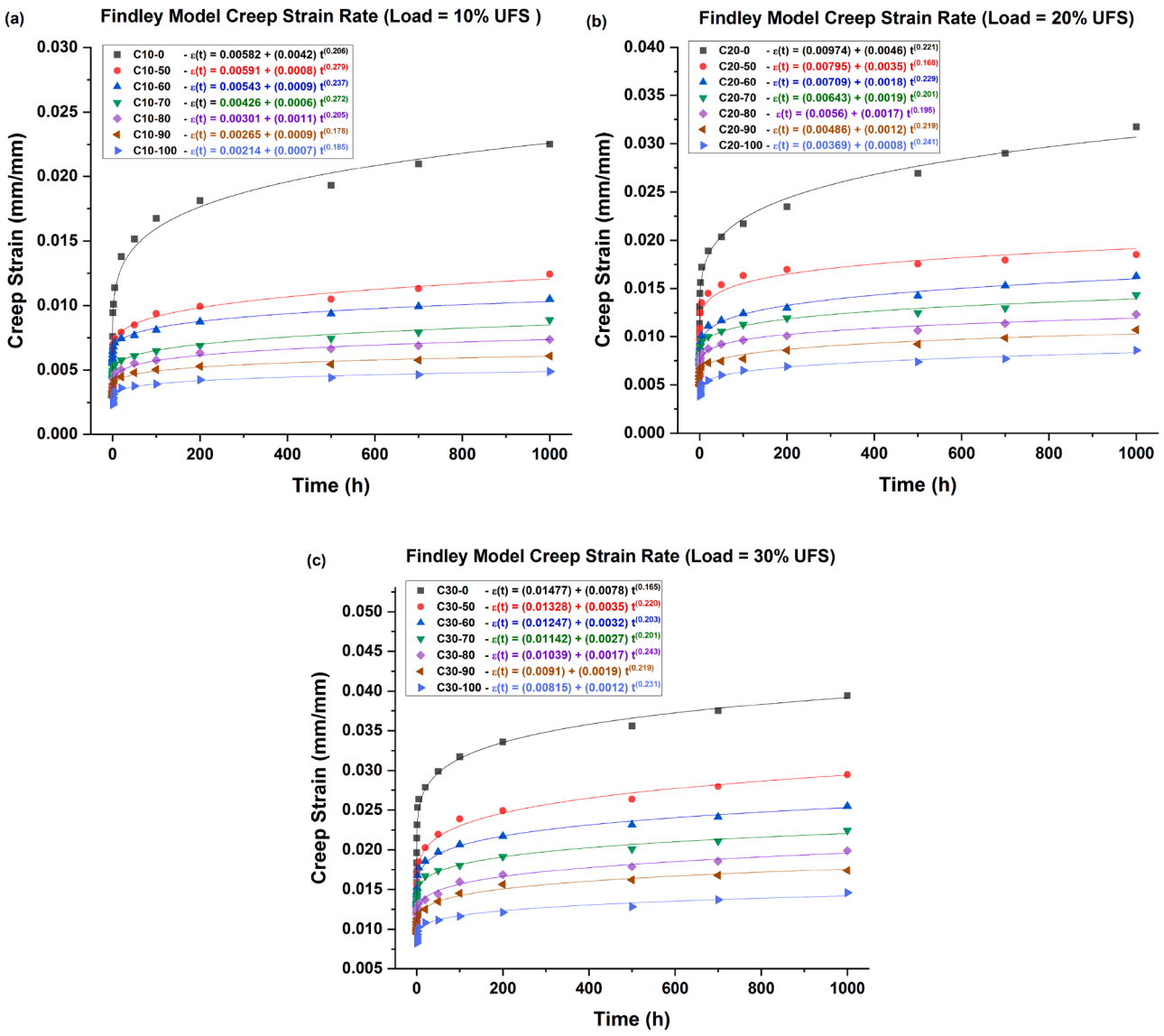

Fig. 10. Comparison of Findley model incorporated creep strain rate of virgin and varying lengths of sleeve reinforced PGFRP composite at (a) 10% (b) 20% (c) 30% load levels of ultimate flexural strength (UFS).

The acceptable percentage error is below the range of 20%–25% and for the purpose of validating numerical data, percentage errors are generally categorized into five classes: highly acceptable (0.0%–9.9% accuracy), good (10%–14.9% accuracy), satisfactory (15%–19.9% accuracy), fair (20–24.9% accuracy), and unacceptable (greater than 25 accuracy) [80,81]. From Table 7 it is evident that the maximum percentage error between the experimental data and Findley model is less than 10% and that there exists higher similarity between the multiple specimens of the composite. This work demonstrated that exact and reliable results from the Findley numerical model were used to validate the experimental data that were plotted to elaborate the creep properties of the pultruded glass fibre reinforced polymer composite used for cross-arm application.

In general, the creep properties of both the samples can be estimated, as shown in Table 8, by applying mathematical equations. Since the model's adjusted regression is highest, the general equations for both specimens are derived from Findley's power law model and provide a good approximation for the creep properties of pultruded glass fibre reinforced polymer composite in a tropical climate.

4. Conclusion

A thorough comparative analysis of the flexural characteristics of the coupon scale virgin and sleeve strengthened pultruded glass fibre reinforced polymer composite has yielded prominent information upon its structural behaviour. The following is a summary of the main conclusions:

- Pultruded glass fibre reinforced polymer composite has been accepted for use in transmission tower applications as a cross-arm material. Experimental research on the flexural load-deflection and flexural creep responses provided important information about the incorporation of structural sleeve reinforcement into the composite material.
- The study evaluated the properties with a sleeve reinforcement of varying lengths and found that the length of the sleeve, and thereby the region encapsulated by it, is directly proportional to the resistance to deformation, ability to withstand higher loads and stress distribution properties.
- The numerical analysis of mechanical properties showed that the sleeve length of just 50% of the span length has increased the

Table 6
Summary of fitted and derived parameters using Findley numerical model.

Specimen	Parameters					
	ϵ_0	a	B	$E_{e,0} = \sigma/\varepsilon_0$ (GPa)	$E_t = \sigma/b$ (GPa)	Adj. R^2
C10-0	0.00582	0.0042	0.206	7.38	10.23	0.9778
C20-0	0.00947	0.0046	0.221	9.08	18.69	0.9887
C30-0	0.01477	0.0078	0.165	8.73	16.54	0.9797
Average		0.0055	0.197	8.40	15.15	0.9821
C10-50	0.00591	0.0008	0.279	7.27	53.74	0.9897
C20-50	0.00795	0.0035	0.168	10.82	24.57	0.9848
C30-50	0.01328	0.0035	0.220	9.71	36.85	0.9893
Average		0.0026	0.222	9.27	38.39	0.9879
C10-60	0.00543	0.0009	0.237	7.92	47.77	0.9870
C20-60	0.00709	0.0018	0.229	12.13	47.77	0.9881
C30-60	0.01247	0.0032	0.203	10.34	40.31	0.9835
Average		0.0019	0.223	10.13	45.28	0.9862
C10-70	0.00426	0.0006	0.272	10.09	71.65	0.9836
C20-70	0.00643	0.0019	0.201	13.37	45.26	0.9759
C30-70	0.01142	0.0027	0.201	11.30	47.77	0.9864
Average		0.0017	0.225	11.59	54.89	0.9820
C10-80	0.00301	0.0011	0.205	14.28	39.08	0.9831
C20-80	0.00560	0.0017	0.195	15.36	50.58	0.9788
C30-80	0.01039	0.0017	0.243	12.41	75.87	0.9907
Average		0.0015	0.214	14.02	55.18	0.9842
C10-90	0.00265	0.0009	0.178	16.22	47.77	0.9720
C20-90	0.00486	0.0012	0.219	17.69	71.66	0.9791
C30-90	0.00910	0.0019	0.219	14.17	67.89	0.9902
Average		0.0013	0.205	16.03	62.44	0.9804
C10-100	0.00214	0.0007	0.185	20.09	61.41	0.9739
C20-100	0.00369	0.0008	0.241	23.30	107.49	0.9885
C30-100	0.00815	0.0012	0.231	15.83	107.49	0.9848
Average		0.0009	0.219	19.74	92.13	0.9824

Table 7
Comparison of instantaneous elastic strain values between experimental data and Findley numerical model.

Specimen	Instantaneous Elastic Strain, ϵ_0 (x 10^{-3})		Percentage Error (%)
	Experimental data	Findley model	
C10-0	6.25	5.82	6.88
C20-0	9.86	9.47	3.95
C30-0	15.86	14.77	6.87
C10-50	6.01	5.91	1.66
C20-50	8.37	7.95	5.01
C30-50	14.10	13.28	5.81
C10-60	5.53	5.43	1.80
C20-60	7.45	7.09	4.83
C30-60	13.14	12.47	5.09
C10-70	4.25	4.26	0.23
C20-70	6.81	6.43	5.58
C30-70	11.86	11.42	3.70
C10-80	3.19	3.01	5.64
C20-80	5.85	5.60	4.27
C30-80	10.58	10.39	1.79
C10-90	2.79	2.65	5.01
C20-90	4.89	4.86	0.61
C30-90	9.46	9.10	3.80
C10-100	2.32	2.14	7.75
C20-100	3.85	3.69	4.15
C30-100	8.25	8.15	1.21

Young's modulus of the material by 67.53%, which further leads to a maximum increase of 178.21% for the sleeve length of 100% of the span length. The sleeve installation has also proven to enhance the transverse mechanical properties in addition to the longitudinal mechanical properties, which makes it more desirable to be utilized in actual scale cross-arm structures.

- The sleeve strengthened pultruded glass fibre reinforced polymer composite has more stable creep properties as compared to the virgin counterpart by fostering a strong viscoelastic region under loading. This phenomenon is yet again directly proportional to the length of the sleeve reinforcement as the surface endured by loading is larger leading to much higher stress distribution, thereby leading to reduced creep strain and ultimately helps achieve longer functional service life of the cross-arms.
- The creep life enhancement can visualized by observing a tremendous increase in the Young's modulus of sleeve retrofitted pultruded glass fibre reinforced polymer composite with 100% of span length by about 138.05% as compared to its virgin counterpart.
- The creep results are further validated using the Findley numerical model and is found to be in compliance with the experimental data and a general mathematical formulae have have been derived from Findley model, for virgin and sleeve reinforced composite, in order to forecast their creep properties.

Table 8
Generalized equation within elastic limit.

Specimen	Equation to forecast creep response
Virgin	$\epsilon(t) = 5.53(10^{-3})t^{0.1973} + \frac{\sigma}{E}$
50% sleeve	$\epsilon(t) = 2.60(10^{-3})t^{0.2223} + \frac{\sigma}{E}$
60% sleeve	$\epsilon(t) = 1.96(10^{-3})t^{0.2230} + \frac{\sigma}{E}$
70% sleeve	$\epsilon(t) = 1.73(10^{-3})t^{0.2246} + \frac{\sigma}{E}$
80% sleeve	$\epsilon(t) = 1.50(10^{-3})t^{0.2143} + \frac{\sigma}{E}$
90% sleeve	$\epsilon(t) = 1.33(10^{-3})t^{0.2053} + \frac{\sigma}{E}$
100% sleeve	$\epsilon(t) = 0.90(10^{-3})t^{0.2190} + \frac{\sigma}{E}$

Essentially, the proposed enhancement in creep characteristics of the sleeve fastened pultruded glass fibre reinforced polymer composite are validated by this investigation. Under real-world circumstances, incorporating this structural improvement seems to be a workable and most feasible method for boosting the cross-arm's strength and lifespan. However, incorporation and evaluation at full-scale level would mark the onset of the potential future research along with the focus on financial and environmental sustainability would add additional value to this application.

CRediT authorship contribution statement

Vijayvignesh Namasivayam Sukumaar: Writing – review & editing, Writing – original draft, Methodology, Investigation, Formal analysis, Data curation, Conceptualization. **Mohamad Ridzwan Ishak:** Visualization, Validation, Supervision, Resources, Project administration, Funding acquisition. **Mohd Na'Im Abdullah:** Validation, Supervision, Project administration, Investigation. **Mohamed Yusoff Mohd Zuhri:** Visualization, Supervision, Software, Project administration. **Muhammad Asyraf Muhammad Rizal:** Visualization, Validation, Project administration, Investigation.

Declaration of competing interest

The authors declare that they have no known competing financial interests or personal relationships that could have appeared to influence the work reported in this paper.

Acknowledgements

This research work was funded by Universiti Putra Malaysia (UPM) for financial support under Geran Inisiatif Putra Siswazah (GP-IPS): GP-IPS/2023/9743400 to carry out all research activities. The authors are also very thankful to Department of Aerospace Engineering, Faculty of Engineering, UPM and Aerospace Malaysia Research Centre (AMRC), UPM for providing space and facilities for the project.

Supplementary materials

Supplementary material associated with this article can be found, in the online version, at doi:10.1016/j.rineng.2024.103735.

Data availability

No data was used for the research described in the article.

References

[1] S.S.S. Ali, M.R. Razman, A. Awang, The nexus of population, GDP growth, electricity generation, electricity consumption and carbon emissions output in Malaysia, Int. J. Energy Econ. Policy 10 (3) (2020) 84–89, https://doi.org/10.32479/ijeep.8987.

[2] M.R.M. Asyraf, M.R. Ishak, S.M. Sapuan, N. Yidris, Conceptual design of creep testing rig for full-scale cross arm using TRIZ-Morphological chart-analytic network process technique, J. Mater. Res. Technol. 8 (6) (2019) 5647–5658, https://doi.org/10.1016/j.jmrt.2019.09.033.

[3] M.R.M. Asyraf, M.R. Ishak, S.M. Sapuan, N. Yidris, R.A. Ilyas, M. Rafidah, M. R. Razman, Evaluation of design and simulation of creep test rig for full-scale crossarm structure, Adv. Civil Eng. 2020 (1) (2020) 6980918, https://doi.org/10.1155/2020/6980918.

[4] C. Bhowmik, K. Gupta, P. Chakraborti, Stability analysis of glass fibre polyamide composite transmission tower, J. Reinf. Plast. Compos. 39 (23-24) (2020) 918–931, https://doi.org/10.1177/073168442093735.

[5] W. Lin, Y. Wang, Y. Aider, M. Rostaghi-Chalaki, K. Yousefpour, J. Kluss, W. Hu, Analysis of damage modes of glass fiber composites subjected to simulated lightning strike impulse voltage puncture and direct high voltage AC puncture, J. Compos. Mater. 54 (26) (2020) 4067–4080, https://doi.org/10.1177/0021998320927736.

[6] A. Syamsir, A. Nadhirah, D. Mohamad, S. Beddu, M.R.M. Asyraf, Z. Itam, V. Anggraini, Performance analysis of full assembly glass fiber-reinforced polymer composite cross-arm in transmission tower, Polymers 14 (8) (2022) 1563, https://doi.org/10.3390/polym14081563.

[7] D.A. Souto-Silvar, A. Álvarez-García, A. Díaz-Díaz, F.J. Rodríguez-Dopico, J. López-Beceiro, Application of the time–temperature superposition principle to predict long-term behaviour of an adhesive for use in shipbuilding, Arab. J. Sci. Eng. 49 (2) (2024) 2345–2355, https://doi.org/10.1007/s13369-023-08219-4.

[8] M.A.S. Bahri, M.M. Ratnam, H.A. Khalil, Functionally graded wood filler–recycled polypropylene composite: effect of mechanical loading on deflection of cantilever beam, Adv. Compos. Lett. 29 (2020), https://doi.org/10.1177/2633366X20922856, 2633366X20922856.

[9] R.A. Ilyas, S.M. Sapuan, A. Atiqah, R. Ibrahim, H. Abral, M.R. Ishak, H. Ya, Sugar palm (Arenga pinnata [Wurmb.] Merr) starch films containing sugar palm nanofibrillated cellulose as reinforcement: water barrier properties, Polym. Compos. 41 (2) (2020) 459–467, https://doi.org/10.1002/pc.25379.

[10] G. Rameshkannan, S. Ramesh Babu, Effect of alkalization on physical, chemical, morphological and mechanical properties of arial root Ficus amplissima fibre, J. Natur. Fibers 19 (15) (2022) 12129–12143, https://doi.org/10.1080/15440478.2022.2051671.

[11] M.R.M. Asyraf, M.R. Ishak, S.M. Sapuan, N. Yidris, Conceptual design of multi-operation outdoor flexural creep test rig using hybrid concurrent engineering approach, J. Mater. Res. Technol. 9 (2) (2020) 2357–2368, https://doi.org/10.1016/j.jmrt.2019.12.067.

[12] R.A. Ilyas, S.M. Sapuan, M.S.N. Atikah, M.R.M. Asyraf, S.A. Rafiqah, H.A. Aisyah, M.N.F. Norrrahim, Effect of hydrolysis time on the morphological, physical, chemical, and thermal behavior of sugar palm nanocrystalline cellulose (Arenga pinnata (Wurmb.) Merr), Textile Res. J. 91 (1-2) (2021) 152–167, https://doi.org/10.1177/0040517520932339.

[13] A.N. Johari, M.R. Ishak, Z. Leman, M.Z.M. Yusoff, M.R.M. Asyraf, Influence of CaCO3 in pultruded glass fiber/unsaturated polyester resin composite on flexural creep behavior using conventional and time-temperature superposition principle methods, Polimery. 65 (2020), https://doi.org/10.14314/polimery.2020.11.6.

[14] M.R.M. Asyraf, M.R. Ishak, S.M. Sapuan, N. Yidris, Comparison of static and long-term creep behaviors between balau wood and glass fiber reinforced polymer composite for cross-arm application, Fibers Polym. 22 (2021) 793–803, https://doi.org/10.1007/s12221-021-0512-1.

[15] M.M. Attia, A.A. El-Latief, M.A. Eita, Performance of RC beams with novelty GFRP under the bending load: an experimental and FE study, Case Stud. Construct. Mater. 18 (2023) e02000, https://doi.org/10.1016/j.cscm.2023.e02000.

[16] M. Ibrahim, A. Asadian, K. Galal, A simplified approach for design of steel-GFRP hybrid reinforced concrete sections, Eng. Struct. 278 (2023) 115352, https://doi.org/10.1016/j.engstruct.2022.115352.

[17] W. Deng, L. Dan, D. Jia, J. Lei, H. Ji, Y. Zhang, Steel–aluminum screw–thread pair tightening mechanism and fastening axial force conversion efficiency, Results Eng. 22 (2024) 102049, https://doi.org/10.1016/j.rineng.2024.102049.

[18] A. Atiqah, M. Jawaid, S.M. Sapuan, M.R. Ishak, M.N.M. Ansari, R.A. Ilyas, Physical and thermal properties of treated sugar palm/glass fibre reinforced thermoplastic polyurethane hybrid composites, J. Mater. Res. Technol. 8 (5) (2019) 3726–3732, https://doi.org/10.1016/j.jmrt.2019.06.032.

[19] A. Sombatmai, K. Tapracharoen, V. Uthaisangsuk, S. Msolli, P. Promoppatum, Post-yielding and failure mechanism of additively manufactured triply periodic minimal surface lattice structures, Results Eng. (2024) 102364, https://doi.org/10.1016/j.rineng.2024.102364.

[20] M.R.M. Asyraf, M. Rafidah, E. Madenci, Y.O. Özkılıç, C. Aksoylu, M.R. Razman, T. Khan, Creep properties and analysis of cross arms' materials and structures in latticed transmission towers: current progress and future perspectives, Materials 16 (4) (2023) 1747, https://doi.org/10.3390/ma16041747.

[21] M.R.M. Asyraf, M. Rafidah, M.R. Ishak, S.M. Sapuan, N. Yidris, R.A. Ilyas, M. R. Razman, Integration of TRIZ, Morphological Chart and ANP method for development of FRP composite portable fire extinguisher, Polym. Compos. 41 (7) (2020) 2917–2932, https://doi.org/10.1002/pc.25587.

[22] S.A. Othman, N.N. Nasir, N.F.A.N. Azman, Natural fibre for composite structural application. Structural Integrity and Monitoring for Composite Materials, 2023, pp. 165–178, https://doi.org/10.1007/978-981-19-6282-0_10.

[23] A.B.M. Supian, M.R.M. Asyraf, A. Syamsir, Q. Ma, K.Z. Hazrati, M.N.M. Azlin, S.M. K. Thiagamani, Kenaf/glass fiber-reinforced polymer composites: pioneering sustainable materials with enhanced mechanical and tribological properties, Polym. Compos. (2024), https://doi.org/10.1002/pc.28785.

[24] L.F. Ng, M.Y. Yahya, C. Muthukumar, J. Parameswaranpillai, Q. Ma, M. R. Muhammad Asyraf, R. Abdul Majid, Mechanical characterization, water absorption, and thickness swelling of lightweight pineapple leaf/ramie fabric-reinforced polypropylene hybrid composites, Polymers 16 (13) (2024) 1847, https://doi.org/10.3390/polym16131847.

[25] K. Gurram, P N, Finite element analysis of reinforced concrete beams strengthened with hybrid fiber reinforced polymer systems using ANSYS, Curr. Mater. Sci.e 17 (3) (2024) 256–265, https://doi.org/10.2174/2666145416666230504143055.

[26] M.R.M. Asyraf, M.R. Ishak, S.M. Sapuan, N. Yidris, R.M. Shahroze, A.N. Johari, R. A. Ilyas, Creep test rig for cantilever beam: fundamentals, prospects and present views, J. Mech. Eng. Sci. 14 (2) (2020) 6869–6887, https://doi.org/10.15282/jmes.14.2.2020.26.0538.

[27] M.R.M. Asyraf, M.R. Ishak, M.R. Razman, M. Chandrasekar, Fundamentals of creep, testing methods and development of test rig for the full-scale crossarm: a review, J. Teknol. 81 (4) (2019), https://doi.org/10.11113/jt.v81.13402.

[28] M.R.M. Asyraf, M.R. Ishak, S.M. Sapuan, N. Yidris, R.A. Ilyas, Woods and composites cantilever beam: a comprehensive review of experimental and numerical creep methodologies, J. Mater. Res. Technol. 9 (3) (2020) 6759–6776, https://doi.org/10.1016/j.jmrt.2020.01.013.

[29] M. Sattar, A.R. Othman, S. Kamaruddin, M. Azad Alam, M. Azeem, Creep parameters determination by omega model to Norton bailey law by regression analysis for austenitic steel ss-304, Solid State Phenomena 324 (2021) 188–197, https://doi.org/10.4028/www.scientific.net/SSP.324.188.

[30] G. Kalyani, N. Pannirselvam, Experimental and numerical investigations on RC beams flexurally strengthened utilizing hybrid FRP sheets, Results Eng. 19 (2023) 101337, https://doi.org/10.1016/j.rineng.2023.101337.

[31] M. Katouzian, S. Vlase, M. Marin, A. Öchsner, Creep response of fiber-reinforced composites: a review, Discover Mech. Eng. 1 (1) (2022) 3, https://doi.org/10.1007/s44245-022-00003-2.

[32] A.L. Amir, M.R. Ishak, N. Yidris, M.Y.M. Zuhri, Flexural creep response of honeycomb sandwich pultruded GFRP composite cross-arm: obtaining full-scale viscoelastic moduli and creep coefficients, J. Mater. Res. Technol. 29 (2024) 225–241, https://doi.org/10.1016/j.jmrt.2024.01.091.

[33] A.L. Amir, M.R. Ishak, N. Yidris, M.Y.M. Zuhri, M.R.M. Asyraf, M.R. Razman, Z. Ramli, Full-scale evaluation of creep coefficients and viscoelastic moduli in honeycomb sandwich pultruded GFRP composite cross-arms: experimental and numerical study, Results Eng. 21 (2024) 101850, https://doi.org/10.1016/j.rineng.2024.101850.

[34] K. Mohammed, R. Zulkifli, M.F.M. Tahir, T.S. Gaaz, A study of mechanical properties and performance of bamboo fiber/polymer composites, Results Eng. (2024) 102396, https://doi.org/10.1016/j.rineng.2024.102396.

[35] C.Y. Bachhav, P.D. Sonawwanay, M. Naik, D.G. Thakur, Experimental and FEA analysis of flexural properties of 3D printed parts, Mater. Today (2023), https://doi.org/10.1016/j.matpr.2023.02.262.

[36] R. Movahedifar, A. Royal, M.E. Torbaghan, N. Metje, D. Chapman, Numerically simulating the interconnected nature of the road-soil-pipe infrastructure, Results Eng. 23 (2024) 102537, https://doi.org/10.1016/j.rineng.2024.102537.

[37] N. Pannirselvam, J.S. Sudarsan, S. Nithiyanantham, Follow effect of low cost glass fibre reinforced polymer (GFRP) on the performance of concentrically loaded concrete column, Vietnam J. Sci. Technol. 61 (5) (2023) 830–843, https://doi.org/10.15625/2525-2518/18079.

[38] M.R.M. Asyraf, A. Syamsir, H. Bathich, Z. Itam, A.B.M. Supian, S. Norhisham, M.Z. A. Rashid, Effect of fibre layering sequences on flexural creep properties of kenaf fibre-reinforced unsaturated polyester composite for structural applications, Fibers Polym. 23 (11) (2022) 3232–3240, https://doi.org/10.1007/s12221-022-4386-7.

[39] S.A. Hassan, A.N. Hanoon, A.A. Abdulhameed, Push-out test of eco-friendly steel-concrete–steel composite sections enhanced by polypropylene fibers: an experimental study and statistical analysis, Results Eng. 23 (2024) 102393, https://doi.org/10.1016/j.rineng.2024.102393.

[40] Bneni, M. K., & Ashour, S. H. (2023). Modelling and simulation of flexural behavior for reinforced concrete beams using ANSYS. https://doi.org/10.54172/mx8n6k70.

[41] R. Liang, Y. Huang, Development length and bond behavior of lap-spliced reinforcement in ultra-high performance concrete beams, Eng. Struct. 291 (2023) 116354, https://doi.org/10.1016/j.engstruct.2023.116354.

[42] I.N.C.E. Gulhan, Effect of link length in retrofitted RC frames with Y eccentrically braced frame, Steel Compos. Struct. 43 (5) (2022) 553–564, https://doi.org/10.12989/scs.2022.43.5.553.

[43] V. Chenrayan, G. Gebremaryam, K. Shahapurkar, K. Mani, Y. Fouad, M.A. Kalam, B.S. Abusahmin, Experimental and numerical assessment of the flexural response

of banana fiber sandwich epoxy composite, Sci. Rep. 13 (1) (2023) 18156, https://doi.org/10.1038/s41598-023-45460-1.
[44] Y. Shen, D.J. Branscomb, A method to measure effective flexural and transverse shear modulus of composite structures with large aspect ratio, Exp. Mech. 62 (6) (2022) 1051–1056, https://doi.org/10.1007/s11340-022-00845-7.
[45] C. Wang, H. Wang, Y. Guo, D. Mohotti, P.J. Hazell, Correlations between moisture expansion and flexural properties of bamboo strips in response to different loading rates, Eur. J. Wood Wood Prod. (2024) 1–12, https://doi.org/10.1007/s00107-024-02091-1.
[46] M. Caballero-Jorna, M. Roig-Flores, P. Serna, Influence of short-term operating temperatures on compression and flexural behaviour of macro synthetic and steel fibre reinforced concretes, J. Build. Eng. 67 (2023) 105919, https://doi.org/10.1016/j.jobe.2023.105919.
[47] A. Alhayek, A. Syamsir, A.B.M. Supian, F. Usman, Lifespan prediction of glass fiber reinforced polymers subjected to flexural creep and elevated temperatures using analytical and numerical analyses, Polym. Compos. (2024), https://doi.org/10.1002/pc.28961.
[48] H. Peng, Z. Hou, X. Chen, T. Li, J. Luo, X. Li, Effect of temperature and cyclic loading on stress relaxation behavior of Ti–6Al–4V titanium alloy, Mater. Sci. Eng. A 824 (2021) 141789, https://doi.org/10.1016/j.msea.2021.141789.
[49] A.L. LourenÇo, N. De Jager, C. Prochnow, D.A.M. Dutra, C.J Kleverlaan, Young's modulus and Poisson ratio of composite materials: influence of wet and dry storage, Dent. Mater. J. 39 (4) (2020) 657–663, https://doi.org/10.4012/dmj.2019-165.
[50] H.T. Tai Nguyen, T.T. Do, V.T. Tran, T.N. Phan, T.A. Pham, M.L. Nguyen, Determination of creep compliance of asphalt mixtures at intermediate and high temperature using creep-recovery test, Road Mater. Pavement Des. 22 (sup1) (2021) S514–S535, https://doi.org/10.1080/14680629.2021.1908407.
[51] W. Yin, Z. Zhao, H. Lin, P. Ma, Advances in creep behaviors of textile composites, Appl. Compos. Mater. 30 (6) (2023) 1949–1978, https://doi.org/10.1007/s10443-023-10154-4.
[52] B. Xu, B. Van Den Hurk, S.J. Lugger, R. Blok, P. Teuffel, Creep analysis of the flax fiber-reinforced polymer composites based on the time–temperature superposition principle, Sci. Eng. Compos. Mater. 30 (1) (2023) 20220218, https://doi.org/10.1515/secm-2022-0218.
[53] C.H. Ndong Bidzo, C.F. Pambou Nziengui, S. Ikogou, B. Kaiser, R. Moutou Pitti, Mechanical properties of Glued-laminated timber made up of mixed tropical wood species, Wood Mater. Sci. Eng. 17 (6) (2022) 809–822, https://doi.org/10.1080/17480272.2021.1960422.
[54] M. Amjadi, A. Fatemi, Creep behavior and modeling of high-density polyethylene (HDPE), Polym. Test. 94 (2021) 107031, https://doi.org/10.1016/j.polymertesting.2020.107031.
[55] A. Chiocca, M. Sgamma, F. Frendo, A closed-form solution for evaluating the Findley critical plane factor, Eur. J. Mech.-A/Solids 105 (2024) 105274, https://doi.org/10.1016/j.euromechsol.2024.105274.
[56] X. Lu, Z. Zhu, K. Wang, D. Yang, Y. Zhu, C. Dai, Hysteretic behavior of composite beam-reinforced concrete column frame, Results Eng. 23 (2024) 102549, https://doi.org/10.1016/j.rineng.2024.102549.
[57] D. Murugan, N. Pannirselvam, Strengthening of structures using FRP composites fibres, in: International Conference on Civil Engineering Innovative Development in Engineering Advances, Springer Nature Singapore, Singapore, 2023, pp. 519–525, https://doi.org/10.1007/978-981-99-6175-7_46.
[58] A.M.N. Maisara, R.A. Ilyas, S.M. Sapuan, M.R.M. Huzaifah, N.M. Nurazzi, S.O. A Saifulazry, Effect of fibre length and sea water treatment on mechanical properties of sugar palm fibre reinforced unsaturated polyester composites, Int. J. Recent Technol. Eng 8 (2S4) (2019) 510–514, https://doi.org/10.35940/ijrte.B1100.0782S419.
[59] N.M. Nurazzi, A. Khalina, S.M. Sapuan, R.A. Ilyas, S.A. Rafiqah, Z.M. Hanafee, Thermal properties of treated sugar palm yarn/glass fiber reinforced unsaturated polyester hybrid composites, J. Mater. Res. Technol. 9 (2) (2020) 1606–1618, https://doi.org/10.1016/j.jmrt.2019.11.086.
[60] K. Gurram, N. Pannirselvam, Experimental and numerical analysis of tensile and flexure tests on a hybrid Aramid/E glass composites, J. Ceram. Process. Res. 24 (3) (2023) 560–568, https://doi.org/10.36410/jcpr.2023.24.3.560.
[61] R. Gopalan, P. Narayanan, Experimental and numerical investigation of tensile-loaded staggered bolted and hybrid pultruded composite double lap joints, J. Adhes. Sci. Technol. 38 (11) (2024) 1895–1924, https://doi.org/10.1080/01694243.2023.2282825.
[62] G. Kalyani, N. Pannirselvam, Numerical studies on RC beams strengthened with an externally bonded aramid FRP sheets, in: International Conference on Civil Engineering Innovative Development in Engineering Advances, Springer Nature Singapore, Singapore, 2023, pp. 439–447, https://doi.org/10.1007/978-981-99-6175-7_40.
[63] Z. Xiang, Y. Liu, X. Zhou, Z. Wu, X. Hu, Interlayer contact mechanism of the frictional behavior of glass-fiber woven fabrics and improvements of winding characteristics, Compos. Struct. 233 (2020) 111497, https://doi.org/10.1016/j.compstruct.2019.111497.
[64] P.K. Alagesan, T. Dirgantara, A. Jusuf, A. Kumaresan Gladys, Q. Ma, Comparison of the lateral crushing response of thin-walled aluminum-thermoplastic polymer composite cylindrical shells, Mech. Adv. Mater. Struct. (2024) 1–16, https://doi.org/10.1080/15376494.2024.2398732.
[65] R.D. Patil, N. Pannirselvam, Comparative study on the performance of RC frame multistorey with three different FRP reinforcements, in: International Conference on Civil Engineering Innovative Development in Engineering Advances, Springer Nature Singapore, Singapore, 2023, pp. 445–457, https://doi.org/10.1007/978-981-99-6233-4_41.
[66] M. Katouzian, S. Vlase, Creep response of carbon-fiber-reinforced composite using homogenization method, Polymers 13 (2021) 867, https://doi.org/10.3390/polym13060867.
[67] D. Di Lorenzo, S. Rodriguez, V. Champaney, C. Germoso, M. Beringhier, F. Chinesta, Damage identification technique by model enrichment for structural elastodynamic problems, Results Eng. (2024) 102389, https://doi.org/10.1016/j.rineng.2024.102389.
[68] H. Wijaya, S. Bandara, P. Rajeev, E. Gad, J. Shan, Failure assessment of deteriorated steel light poles, Results Eng. 23 (2024) 102621, https://doi.org/10.1016/j.rineng.2024.102621.
[69] F. Hoseinzadeh, S.M. Zabihzadeh, F. Dastoorian, Creep behavior of heat treated beech wood and the relation to its chemical structure, Constr. Build. Mater. 226 (2019) 220–226, https://doi.org/10.1016/j.conbuildmat.2019.07.181.
[70] R.M. Neves, H.L. Ornaghi Jr, F.C. Alves, A.J. Zattera, M. Tom, H.M. Lal, S Thomas, Creep and stress relaxation behavior of functionalized microcrystalline cellulose/epoxy composites, Cellulose 30 (4) (2023) 2197–2216, https://doi.org/10.1007/s10570-022-05020-8.
[71] N. Hao, Y. Wang, Y. Song, S. Ruan, Q. Ma, Z. Wang, Load-bearing behaviors of sandwich plates with non-uniformly distributed grid cores: static compression and bending, J. Mater. Sci. 58 (42) (2023) 16488–16506, https://doi.org/10.1007/s10853-023-09059-1.
[72] B. Rashid, N. Razali, Z. Leman, M. Jawaid, Single fiber test behavior of lignocellulose sugar palm fibers: effect of treatments, Key. Eng. Mater. 925 (2022) 37–46, https://doi.org/10.4028/p-58u653.
[73] D.C.T. Cardoso, K.A. Harries, A viscoelastic model for time-dependent behavior of pultruded GFRP, Constr. Build. Mater. 208 (2019) 63–74, https://doi.org/10.1016/j.conbuildmat.2019.02.155.
[74] P. Kajendran, P. Narayanan, Analytical evaluation of three-dimensional pultruded GFRP semi rigid frame with bracings and mechanical insert, in: AIP Conference Proceedings 3187, AIP Publishing, 2024, https://doi.org/10.1063/5.0236863.
[75] Y.A.O. Xingyou, R.U.A.N. Chuhang, L.I.U. Yafei, L.I.U. Yilin, C.H.E.N. Hou, G.U. O. Yanli, Z.E.N.G. Kaihua, Experiment and design of cold-formed steel equal-leg lipped angle under axial compression, Results Eng. (2024) 102716, https://doi.org/10.1016/j.rineng.2024.102716.
[76] M.A. Riezzo, M. Simmons, B. Russell, F. Sket, V. Martínez, C. González, Dynamic characterisation of interlaminar fracture toughness in carbon fibre epoxy composite laminates, Compos. Part A 126 (2019) 105597, https://doi.org/10.1016/j.compositesa.2019.105597.
[77] P. Kajendran, P. Narayanan, Experimental and finite element investigation on bolted connection in monolithic 3-dimensional cuff with pultruded box section, Eng. Res. Express 6 (2) (2024) 025110, https://doi.org/10.1088/2631-8695/ad4438.
[78] T. D'Antino, M.A. Pisani, Long-term behavior of GFRP reinforcing bars, Compos. Struct. 227 (2019) 111283, https://doi.org/10.1016/j.compstruct.2019.111283.
[79] H.L. Ornaghi Jr, J.H.S. Almeida Jr, F.M. Monticeli, R.M Neves, Stress relaxation, creep, and recovery of carbon fiber non-crimp fabric composites, Compos. Part C 3 (2020) 100051, https://doi.org/10.1016/j.jcomc.2020.100051.
[80] L. Collini, R. Garziera, A. Corvi, G. Cantarelli, Slip strength of COR-TEN and Zn-coated steel preloaded bolted joints, Results Eng. 22 (2024) 102009, https://doi.org/10.1016/j.rineng.2024.102009.
[81] X. Kong, Y. Wang, Q. Yang, R. Yang, Modeling and measurements of creep deformation in a ceramic fiber reinforced metal matrix composite, Compos. Part B (2024) 111926, https://doi.org/10.1016/j.compositesb.2024.111926.